

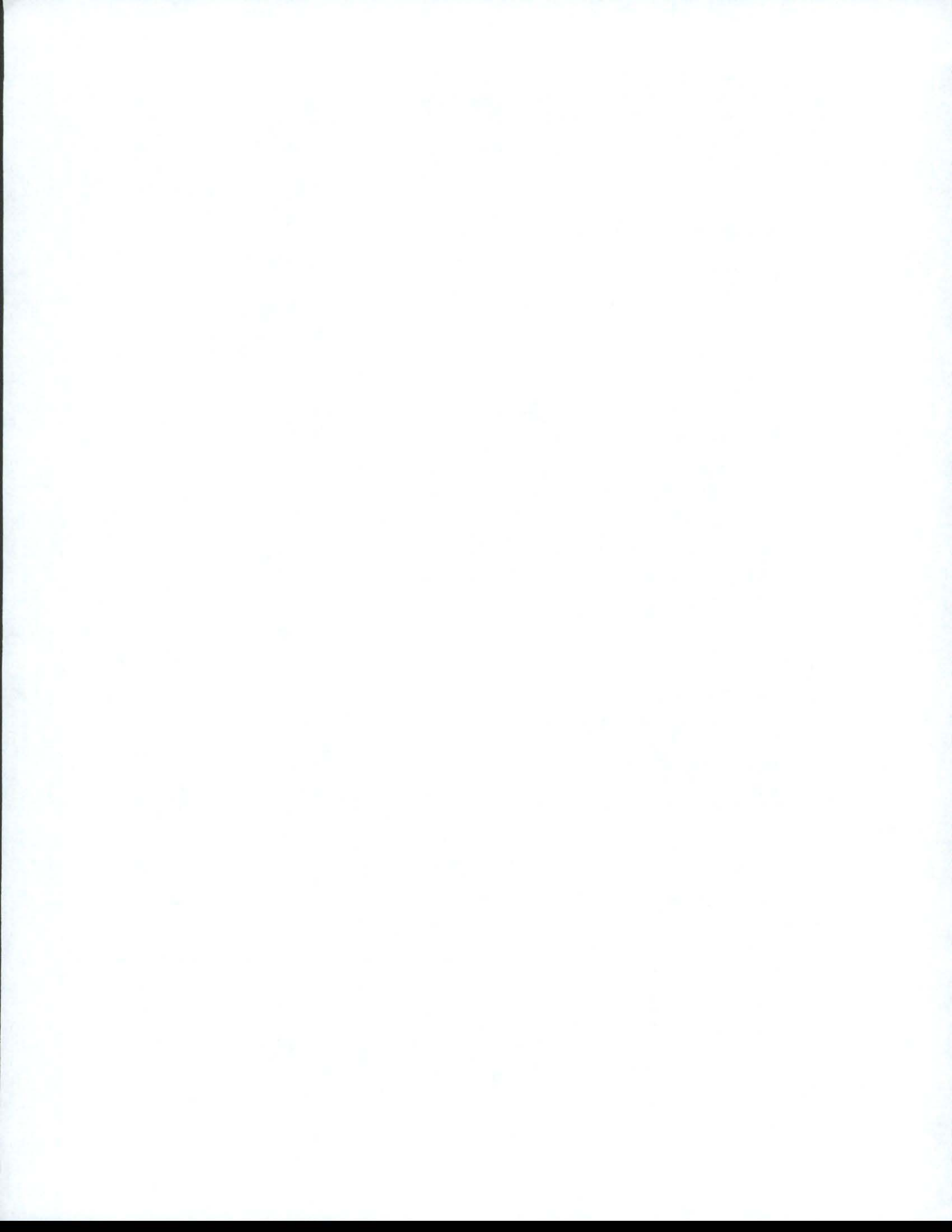
# REPORT DOCUMENTATION PAGE

Form Approved  
OMB No. 0704-0188

Public reporting burden for this collection of information is estimated to average 1 hour per response, including the time for reviewing instructions, searching existing data sources, gathering and maintaining the data needed, and completing and reviewing this collection of information. Send comments regarding this burden estimate or any other aspect of this collection of information, including suggestions for reducing this burden to Department of Defense, Washington Headquarters Services, Directorate for Information Operations and Reports (0704-0188), 1215 Jefferson Davis Highway, Suite 1204, Arlington, VA 22202-4302. Respondents should be aware that notwithstanding any other provision of law, no person shall be subject to any penalty for failing to comply with a collection of information if it does not display a currently valid OMB control number. PLEASE DO NOT RETURN YOUR FORM TO THE ABOVE ADDRESS.

<b>1. REPORT DATE (DD-MM-YYYY)</b> 30 Jan 2009		<b>2. REPORT TYPE</b> Technical Paper		<b>3. DATES COVERED (From - To)</b> 30 Jan 2009-13 April 2009	
<b>4. TITLE AND SUBTITLE</b>  Nonlinear Optical Dynamic Range Compression with Thin-Film Organic Photorefractive Material				<b>5a. CONTRACT NUMBER</b> In-House	
				<b>5b. GRANT NUMBER</b>	
				<b>5c. PROGRAM ELEMENT NUMBER</b>  61102F	
<b>6. AUTHOR(S)</b>  *Bahareh Haji-saeed, John Kierstead, **Jed Khoury, Charles Woods, ***Nasser Peyghambarian				<b>5d. PROJECT NUMBER</b> 2303	
				<b>5e. TASK NUMBER</b> HC	
				<b>5f. WORK UNIT NUMBER</b> 00	
<b>7. PERFORMING ORGANIZATION NAME(S) AND ADDRESS(ES)</b> *Solid State Scientific Corporation, Hollis, NH 03049; **Air Force Research Laboratory, 80 Scott Drive, Hanscom AFB, MA 01731; ***University of Arizona, Optical Sciences, Tucson, AZ 85721				<b>8. PERFORMING ORGANIZATION REPORT</b>	
<b>9. SPONSORING / MONITORING AGENCY NAME(S) AND ADDRESS(ES)</b>  Electromagnetics Technology Division                      Source Code: 437890  Sensors Directorate Air Force Research Laboratory 80 Scott Drive Hanscom AFB MA 01731-2909				<b>10. SPONSOR/MONITOR'S ACRONYM(S)</b>  AFRL/RYHC	
				<b>11. SPONSOR/MONITOR'S REPORT NUMBER(S)</b> AFRL-RY-HS-TR-2010-0040	
<b>12. DISTRIBUTION / AVAILABILITY STATEMENT</b>  DISTRIBUTION A: APPROVED FOR PUBLIC RELEASE; DISTRIBUTION UNLIMITED.					
<b>13. SUPPLEMENTARY NOTES</b> The U.S. Government is joint author of this work and has the right to use, modify, reproduce, release, perform, display, or disclose the work. Published in Proc. of SPIE, Vol. 7340, 73400J, 13 April 2009. Cleared for Public Release by 66ABW-2009-0106, 30 January 2009.					
<b>14. ABSTRACT</b> Nonlinear information processing via two-beam coupling using thin-film organic photorefractive material is demonstrated. The organic material is found to possess superior response time and resolution compared to photorefractive bulk material. The possibility of designing dynamic range compression deconvolution for restoring blurred images embedded in a noisy environment is also demonstrated.					
<b>15. SUBJECT TERMS</b>  Photorefractive optics; Nonlinear optical signal processing; Optical nonlinearities in organic materials					
<b>16. SECURITY CLASSIFICATION OF:</b> Unclassified			<b>17. LIMITATION OF ABSTRACT</b>  SAR	<b>18. NUMBER OF PAGES</b>  23	<b>19a. NAME OF RESPONSIBLE PERSON</b> Bahareh Haji-saeed
<b>a. REPORT</b> Unclassified	<b>b. ABSTRACT</b> Unclassified	<b>c. THIS PAGE</b> Unclassified			<b>19b. TELEPHONE NUMBER (include area code)</b> n/a

Standard Form 298 (Rev. 8-98)  
Prescribed by ANSI Std. Z39.18



# Nonlinear Optical Dynamic Range Compression with Thin-Film Organic Photorefractive Material

Bahareh Haji-saeed<sup>1</sup>, Jed Khoury<sup>1</sup>, Charles L. Woods<sup>1</sup>, John Kierstead<sup>2</sup>, and Nasser Peyghambarian<sup>3</sup>

<sup>1</sup>Air Force Research Laboratory / RYHC, Hanscom Air Force Base, MA 01731

<sup>2</sup>Solid State Scientific Corporation, Hollis, NH 03049

<sup>3</sup>University of Arizona, Optical Sciences, Tucson, Arizona 85721

**Abstract:** Nonlinear information processing via two-beam coupling using thin-film organic photorefractive material is demonstrated. The organic material is found to possess superior response time and resolution compared to photorefractive bulk material. The possibility of designing dynamic range compression deconvolution for restoring blurred images embedded in a noisy environment is also demonstrated.

**Keywords:** Photorefractive optics; Nonlinear optical signal processing; Optical nonlinearities in organic materials

## 1. INTRODUCTION

Imaging in atmospheric turbulence has been a research topic for many years. Currently, there are some well established techniques for image restoration. However, if the atmospheric turbulence becomes a severe scattering medium, most conventional approaches, such as inverse filtering and Wiener filtering (1) (the optimal mean square error image restoration filter), won't be adequate for correcting the captured images.

In addition weather volumes with clouds, fog, smoke, haze, dust, or other dispersed substances can significantly reduce the image quality in the visible spectrum. These situations produce degraded images in conventional cameras when imaging in remote sensing applications.

To overcome the shortcoming with the conventional image restoration approaches, we propose a dynamic range compression image restoration technique using optical two beam coupling (2-4).

Operating these devices in the dynamic range compression regime with high efficiency requires high-gain bulk photorefractive materials (5, 6).

Unfortunately, the response time of all high-gain photorefractive materials is on the order of seconds, making them impractical for real-time signal processing applications. In addition, the resolution in the energy transfer via two-beam coupling with thick holographic material is low for two reasons (6, 7): (1) reflection from the thick hologram, and (2) the dephasing factor, which increases with the thickness of the holographic material. Both the response time and resolution issues can be overcome by using thin film holographic material.

Photorefractive materials in both two-beam coupling and four-wave mixing architectures have been used in a variety of applications, including edge enhancement (8), optical correlation (9), defect enhancement (10), associative memory (11), and image amplification (12).

## 2. BACKGROUND

Here we introduce the two-beam coupling joint Fourier processor. Figure 1 shows the proposed architecture of our two-beam coupling joint Fourier processor.

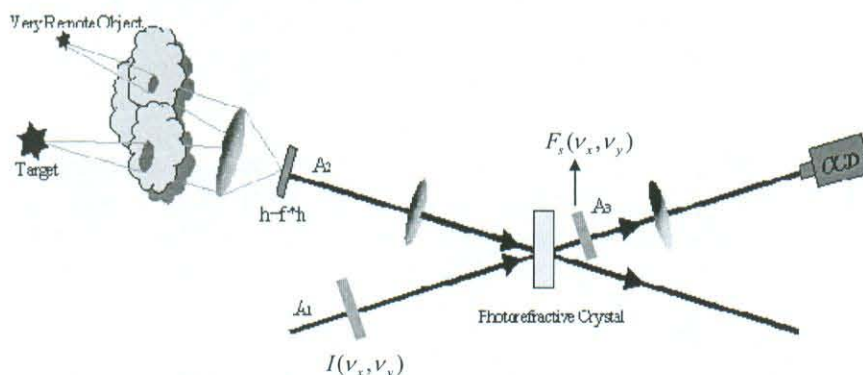


Figure 1. Two-beam coupling joint Fourier processor

A joint image of a remote source and the object is captured via an optically or electrically addressed spatial light modulator for processing. The Fourier transform of the joint image ( $A_2$ ) is used to pump either a clean or a spectrally variant reference beam ( $A_1$ ) via a nonlinear photorefractive element. The CCD camera captures the Fourier transform of the lowpass filtered diffracted beam ( $A_3$ ). This beam contains gray level information for the corrected image and its conjugate. The spectrally variant reference beam is shaped through a beam profiler. A beam profiler is a spatial light modulator (SLM) addressed by the joint spectra envelope through direct measurement. The beam profiler is essential to reduce extremely high beam ratios required to achieve dynamic range compression. The deflected output from the crystal is spatially filtered through an amplitude lowpass filter  $F_s(v_x, v_y)$ . The output of this filter is Fourier transformed to produce the joint spectra gray level recovered information and is given by:

$$A(v_x, v_y) = A(0) \left[ \frac{1 + m/(\lambda f_l)^2 |R(v_x, v_y) + S(v_x, v_y)|^2}{1 + m/(\lambda f_l)^2 |R(v_x, v_y) + S(v_x, v_y)|^2 \exp(-\Gamma l)} \right]^{1/2} F_s(v_x, v_y) \quad (1)$$

where  $v_x$  and  $v_y$  are spatial frequencies,  $m$  is the beam intensity ratio before passage of the signal beam through the transparency bearing objects,  $\lambda$  is the wavelength,  $f_l$  is the focal length,  $\Gamma$  is the intensity coupling constant,  $l$  is the crystal thickness, and  $R$  and  $S$  are H and HF, respectively. According to this equation the nonlinear transfer function of the diffracted beam consists of square-law receiving and

saturation nonlinearity (3, 4). The square-law receiving is responsible for mixing the Fourier transform of the blurred image with the impulse response thereby correcting the phase aberration. The saturation nonlinearity associated with energy transfer of two beam coupling is responsible for enhancing both the high frequency components of the image (restoring edge features) and the signal-to-noise ratio when the noise is stronger than the signal (reducing additive noise).

The proposed setup is based on the energy transfer within two beam coupling. The earlier works on energy transfer in two beam coupling via bulk photorefractive material was considered for a beam cleanup device (13). Later attempts with thinner material introduced in reference 14, it was demonstrated that the energy transfer in two beam coupling functions as an optically addressed spatial light modulator, but with degraded performance. The degraded performance of energy transfer two beam coupling in bulk photorefractive material is anticipated for several reasons:

- (1) The diffracted very narrow beam (delta function) from a bulk material is a broad beam (broad impulse response) (15).
- (2) The dephasing in Bragg matched conditions (16, 17) is asymmetric for both reflection and transmission geometry. The asymmetry in the dephasing factor is more severe in the transmission geometry than in the reflection geometry. Maximum dephasing happens in the interfering beams plane while the minimum dephasing happens perpendicular to the interfering beams plane. This asymmetry diminishes fully in the back propagating geometry. The effect of the dephasing on the efficiency of the energy transfer is less for thin holographic material.

Therefore, in order to avoid the asymmetric dephasing factor and the broad impulse response, we decided to use thin film organic photorefractive material. The above arguments indicate that the reflection and the counter propagation geometries should be able to give us the best results in terms of resolution. However, this is not necessary true, because the efficiency of both reflection and counter propagation geometries are low which might not provide enough dynamic range compression needed for performing the compression deconvolution.

### 3. EXPERIMENTAL SETUPS AND RESULTS

Prior to demonstrating the dynamic range compression deconvolution using two beam coupling, we conducted several tests:

- (1) The two beam coupling energy transfer fidelity in terms of resolution and symmetry as a spatial light modulator as well as a Fourier processor.
- (2) The two beam coupling energy transfer fidelity as a symmetric joint Fourier processor.
- (3) Dynamic range compression capability of two beam coupling for signal to noise improvement.
- (4) Dynamic range compression edge enhancement via compression deconvolution.

#### 3.1 Two beam coupling energy transfer spatial light modulation fidelity

For the first time, we demonstrate high optical quality spatial light modulation using energy transfer in two beam coupling. We tested the spatial light modulation fidelity of two beam coupling using Nitto Denko organic (18) material in both the transmission and reflection geometries as an imager and as a Fourier processor. Figure 2(A, B) show the experimental arrangement for testing spatial modulation fidelity for the transmission and the reflection geometries, respectively. We have also set the spatial

light modulation experiment in the counter-propagating geometry which is essentially the reflection geometry setup with counter propagating write up beams.

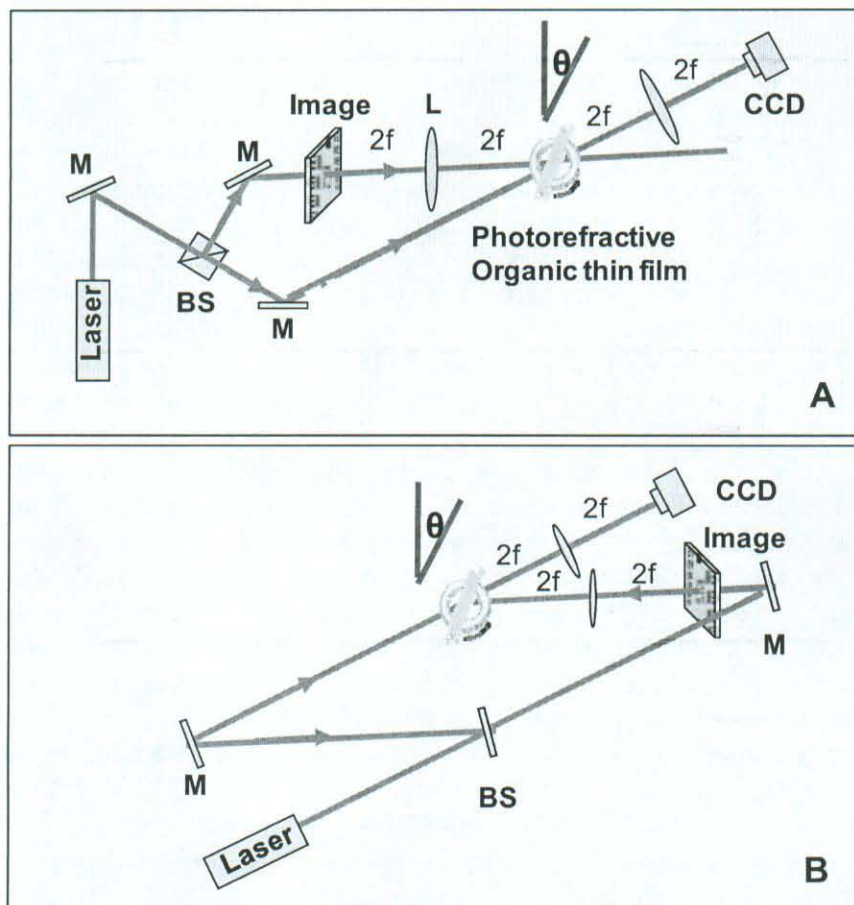


Figure 2. (A) Transmission geometry and (B) Reflection Geometry

The input object was either imaged or Fourier transformed to the organic material through a lens. In the imaging case, a lens with focal point  $f$  was located at a distance of  $2f$  from both the input and the organic material. For the Fourier processing case, the lens was located at a distance of  $f$  from the organic material. It is shown in the figure that the material was tilted  $\theta=40^\circ$  and  $\theta=70^\circ$  for the transmission geometry and the reflection geometry, respectively.

Figure 3(A) shows the output result in the transmission geometry for the imaging case when the input was a US Air Force resolution chart. As it is evident, it was possible to show a high quality modulation of one beam with another beam's information through energy transfer in two-beam coupling.

The Fourier processing capability was tested by Fourier transforming a periodical structure to the organic material. The Fourier transform of a periodical structure is a periodical structure. Modulating a clean beam with a periodical structure via the energy transfer in two beam coupling should give us a periodical structure as well, while the Fourier transformation of this output should be again a periodical structure. Figures 3(B) shows a periodical structure for Fourier processing testing in the transmission geometry. The symmetry in periodical structure testing of the transmission geometry indicates that the two beam coupler can function as an excellent Fourier processor. In contrast, the results in the reflection geometry shows less resolution quality compared to the transmission geometry due to the coupling with internal reflection within the thin film as it is apparent in Figure 3(C). To avoid the internal reflection, we tilted the material by an angle of  $\theta=70^\circ$ . The coupling from the internal reflection was avoided as shown in Figure 3(D); however, the efficiency of the energy transfer was significantly reduced.

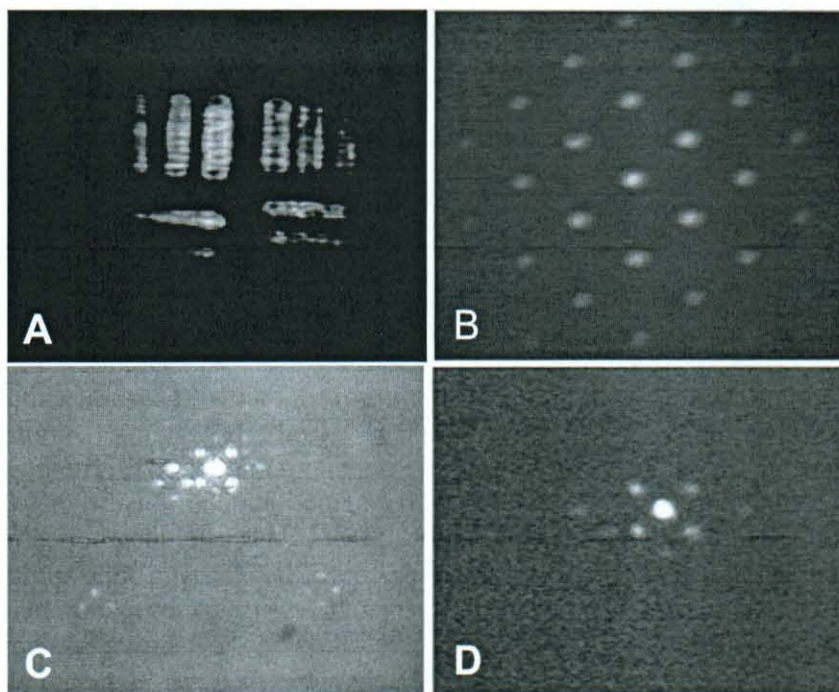


Figure 3. The energy transferred results of (A) a resolution chart, (B) periodical structure for transmission geometry, (C) periodical structure for reflection geometry  $\theta=0$  and (D) periodical structure for reflection geometry  $\theta=70^\circ$

### 3.2 Joint Fourier Processor Symmetric Fidelity

In our previous work, we attempted to perform optical correlation via energy transfer in two beam coupling. Even though it was demonstrated in computer simulation that correlation via two beam coupling has superior performance compared to binary filter and optimal filters; however, these

correlators couldn't been used in joint Fourier processors due to their lack of symmetry in their correlation results. This also applies for deconvolution processors.

For the first time, we demonstrate a symmetric joint Fourier processor using energy transfer in two beam coupling with organic photorefractive materials. In order to test the joint Fourier processor fidelity, we used two circles as the joint input. The correlation between the two circles should be as maximum as possible invariant to the input rotation.

The experimental arrangement for testing the joint Fourier processing fidelity of two-beam coupling in transmission and reflection geometries are shown in Figure 4(A) and 4 (B), respectively. We have also tested the correlation experiment for the counter-propagating geometry.

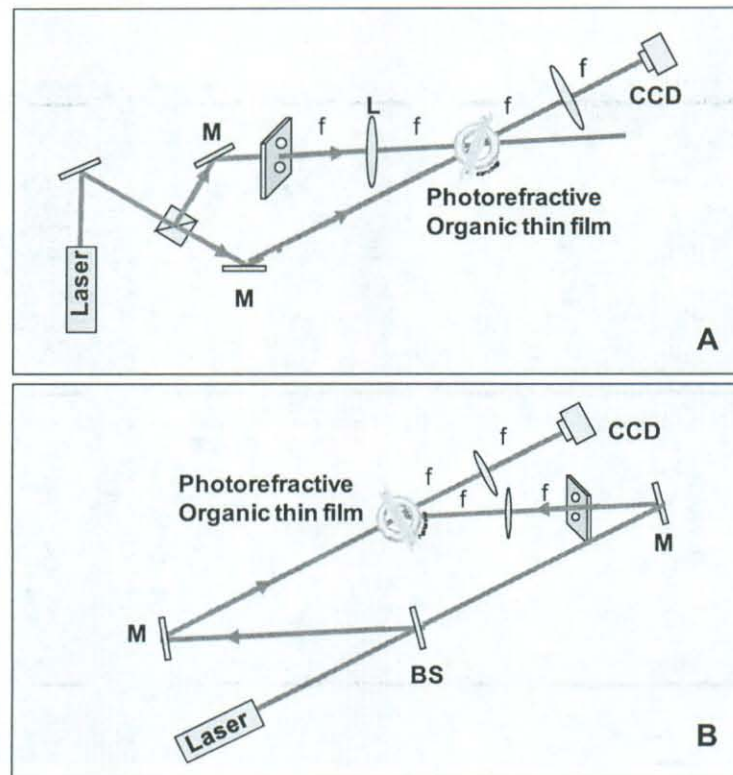
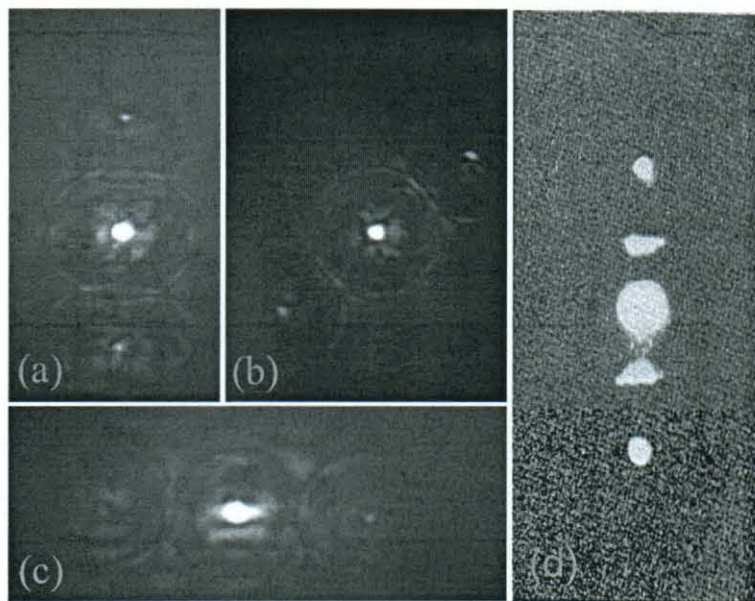


Figure 4. Two-beam coupling JTC in (A) transmission geometry, (B) reflection geometry

The laser beam was collimated and divided to two beams; one beam was passed through a neutral-density filter, while the other beam was passed through a metallic mask with several pairs of circular holes. Each pair represents the signal (s) and the reference (r). This target was chosen to test the correlation fidelity of this scheme for more sophisticated experiments. The signal and the reference beams were jointly Fourier transformed via a lens and were interfered with a clean beam at the organic material plane. The diffracted output from the material (correlation result) was Fourier transformed

and captured via a CCD camera. Figure 5 shows the experimental results of correlating two identical circular holes. Figure 5(a) shows the correlation peaks when the holes are vertically aligned, while figures 2(b) and 2(c) show the results when the mask is rotated  $45^\circ$  and  $90^\circ$ , respectively.



**Figure 5. (a) the correlation peaks when the holes are vertically aligned, (b)  $45^\circ$  rotated, (c)  $90^\circ$  rotated and (d) correlation results using bulk photorefractive material**

It is clear from these results that the correlation peaks can be very narrow and the rings around them can be observed completely if we use the organic thin film material from Nitto Denko, while performing this experiment with bulk photorefractive material would result in broader correlation peaks, with arcs around them instead of rings. This is due to the dephasing and broad impulse response in bulk photorefractive material as discussed before, which is shown in figure 5(d). The fact that we could get correlation results regardless of the target orientation using organic thin film material will allow us to test more complex input images than was possible using bulk photorefractive material.

The theoretical basis of the two-beam coupling joint transform correlator presented in equation (1) was derived using the plane-wave two-beam coupling wave equation solutions. This equation is plotted in figure 6. In the diffusion limit, when a clean beam with spatially constant amplitude is amplified by a beam bearing joint spectra of two images,  $r$  and  $s$ , the output at the crystal (Fourier) plane can be written as equation 1.

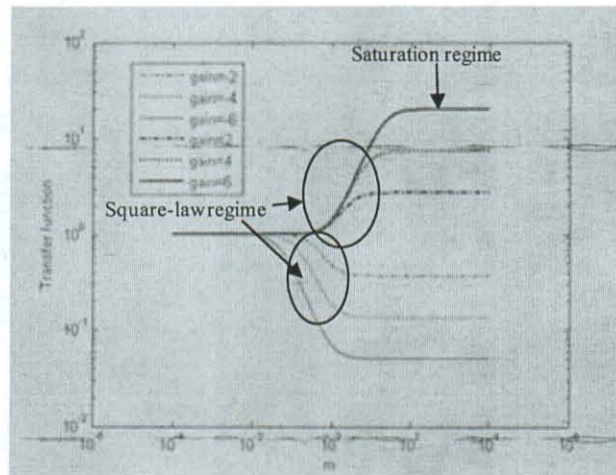


Figure 6. Two-beam coupling input-output nonlinear transfer function

Figure 7 shows the correlation results for reflection geometry. As we discussed before, in order to avoid the internal reflection we tilted the organic film by  $70^\circ$ . Figure below shows this improvement from (a)  $\theta=0^\circ$ , (b)  $\theta=40^\circ$  to (c)  $\theta=70^\circ$ .

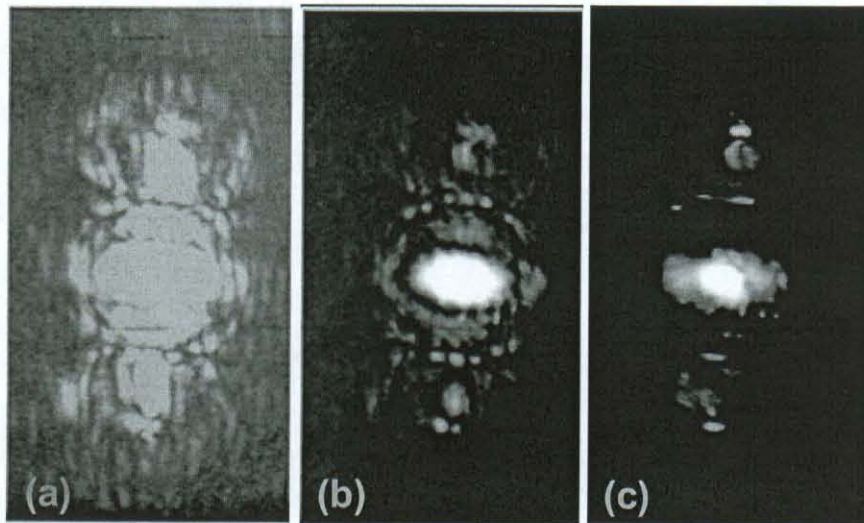


Figure 7. Correlation results in reflection geometry: (a)  $\theta=0^\circ$ , (b)  $\theta=40^\circ$ , and (c)  $\theta=70^\circ$

### 3.3. Dynamic range compression capability for signal to noise improvement

For the first time, we experimentally demonstrate the peak (signal) to noise enhancement of a symmetric noise compression utilizing the dynamic range compression features of two-beam energy transfer. The input-output nonlinear transfer functions via energy transfer in two beam coupling

functions as a limiting square law receiver. At low signal intensities, it functions as a square-law receiver and at high signal intensities; it functions as a hard-clipper and a dynamic range compression device. As demonstrated before, Figure 6 illustrates the two-beam coupling input-output nonlinear transfer function. For a signal embedded in noise, the limiting square-law receiver enhances the signal-to-noise ratio (SNR). The optimal receiving point for enhancing the SNR is when the noise variance is equal to the hard clipping point (threshold value).

Figure 8 shows our experimental setup, in which zero-mean noise was generated by a diffuser for both transmission and reflection geometries. Also, we set up the experiment in counter-propagating geometry which is essentially the reflection geometry with counter propagating writing beams. The noise transmission from the diffused beam to the reference beam was performed via the two-beam coupling energy transfer utilizing Nitto Denko thin-film photorefractive material. The square-law nonlinearity associated with two-beam coupling converts the zero-mean noise to nonzero-mean noise. For a perfect square-law receiver (low beam ratio), 50% of the noise energy is converted to DC, while the rest of the energy remains zero-mean Gaussian noise with double the frequency. The Fourier transform of the noisy diffracted output has a large DC peak within the surrounding high frequency noise. For a low energy noise beam, the square-law operation results in the energy equality of the DC peak and the surrounding noise, while for a high energy noise beam, the dynamic range compression results in: (a) an increase in noise frequency, and (b) an increase in the DC component intensity relative to the surrounding zero-mean noise components.

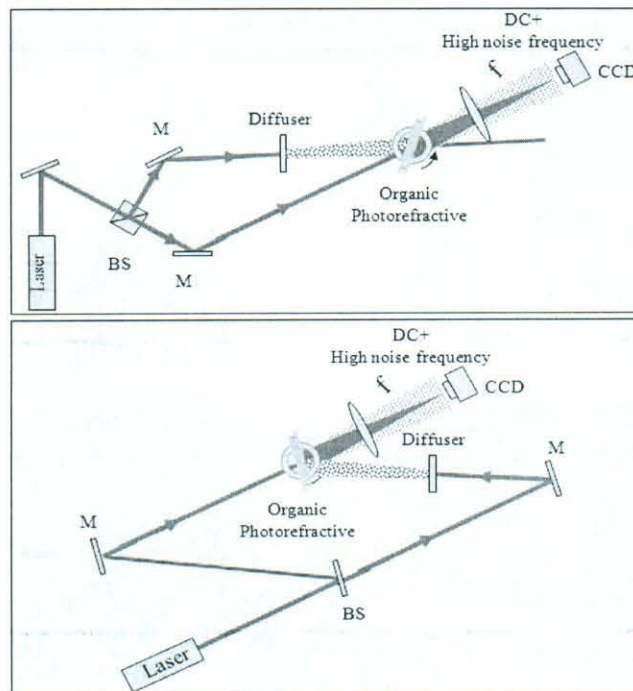


Figure 8. Noise compression experimental setup

Figure 9 shows our experimental results for the Fourier transform of the diffracted noisy output for four different beam ratios. The gray level insets are the captured photos, while the colored images are the pseudo color-coded versions of the original photos. These results were normalized to the exact measured DC intensities. It is evident that the DC peak intensity is the same in all of these images (brown area), while the intensity of the surrounding noise decreases (yellow to blue areas) as the dynamic range compression is increased ( i.e. higher beam ratios).

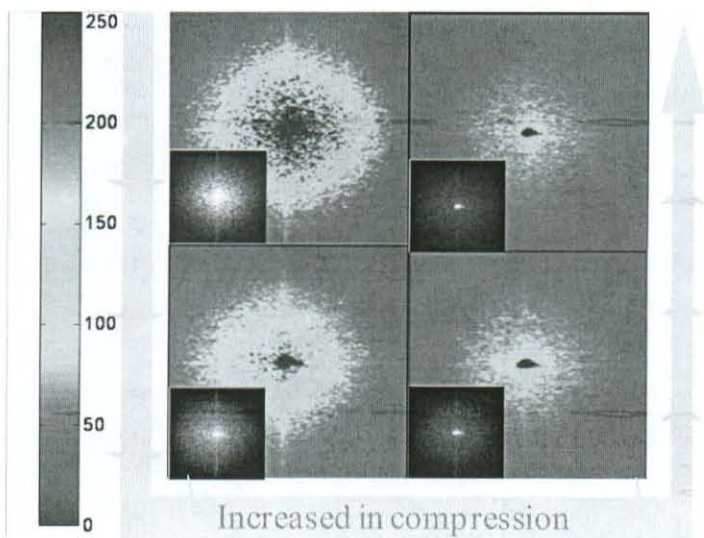


Figure 9. Noise compression experimental results

We performed the same experiment in the reflection geometry; the results were similar except it was hard to conduct the experiment over a large dynamic range. Figure 10 shows results of noise transfer when the experiment was conducted in the reflection geometry.

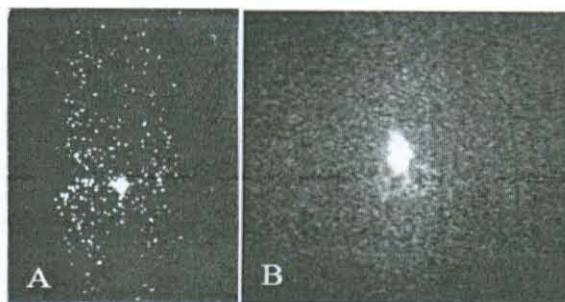


Figure 10. Noise transfer function in the reflection geometry for (A) the bulk material and (B) the Nitto Denko thin film organic material

This figure shows the comparison of the output results from (A) the bulk material and (B) the Nitto Denko thin film organic material. Comparing these results shows that the noise energy transfer around the DC peak at the center is nearly symmetric when the experiment is performed with Nitto Denko thin film organic material and is asymmetric, nearly truncated in the horizontal direction when the bulk material is used.

### 3.4. Dynamic range compression edge-enhancement via two beam coupling energy transfer

Two-beam coupling dynamic compression edge enhancement is a special case of our proposed two-beam coupling nonlinear deconvolution. In the proposed deconvolution technique, a joint image of a point source and a target is captured via an optically or electrically addressed spatial light modulator as shown in figure 11.

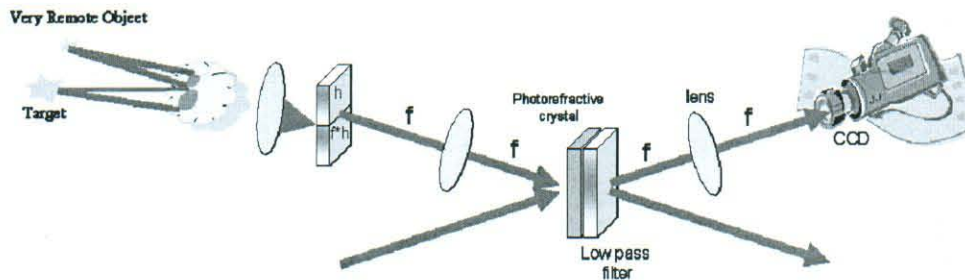


Figure 11. Two-beam coupling nonlinear deconvolution setup

The captured image consists of the impulse response of the distortion medium (the blur function) and the blurred target image. The Fourier transform of the joint image is used to pump either a clean or a spectrally variant reference beam within a nonlinear photorefractive element. The CCD camera captures the Fourier transform of the lowpass filtered diffracted beam. This beam contains the gray level information for the corrected image and its conjugate. The spectrally variant reference beam is shaped through a beam profiler. A beam profiler is a SLM addressed by the joint spectra envelope through direct measurement. The beam profiler is essential to reduce the extremely high beam ratios required to achieve dynamic range compression. The diffracted output from the photorefractive material is spatially filtered through an amplitude lowpass filter,  $F_s(v_x, v_y)$ . The output of this filter is Fourier transformed to produce the gray level recovered information (deconvolution result) as given in equation 1, where  $R$  and  $S$  are  $H$  (blur function) and  $HF$  (blurred image), respectively. According to this equation, the nonlinear transfer function of the diffracted beam consists of square-law receiving and saturation nonlinearity. The square-law receiving is responsible for mixing the Fourier transform of the blurred image with the impulse response, thereby correcting the phase aberration. The saturation nonlinearity associated with the energy transfer in two-beam coupling (Figure 6) is responsible for enhancing both the high frequency components of the image (restoring edge features) and the signal-to-noise ratio when the noise is stronger than the signal (reducing additive noise). For a noiseless image and  $F_s(v_x, v_y) = 1$ , the recovered image is always the edge enhanced version of the original image, regardless of the existence of a blurring function in the system.

Figure 12 shows our edge enhancement experimental setup, in which the photorefractive material is a Nitto Denko organic thin film.

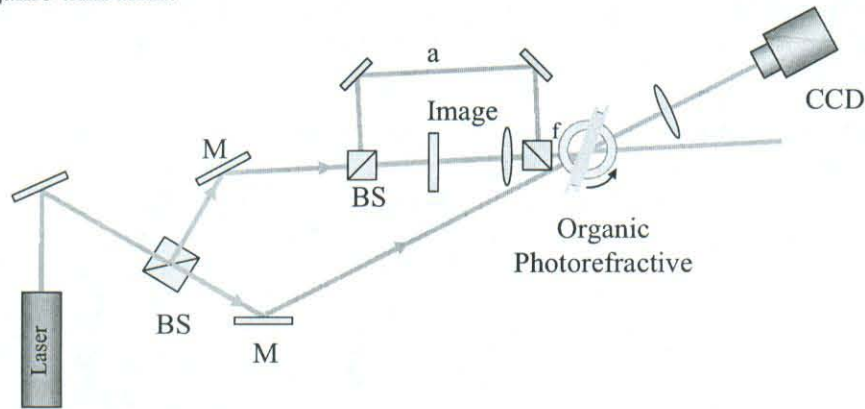


Figure 12. Edge enhancement experimental setup

Here the joint image is not blurred, so the joint input consists of a probe beam (a delta function) and the original image. The output result of this experiment should be the edge enhanced version of the original input, as expected from image restoration with the dynamic range compression deconvolution experiment. The result is shown in Figure 13, where (A) is the input image and (B) is the edge enhanced version. The output result (the edges quality) can significantly improve if the clean probe beam is expanded.

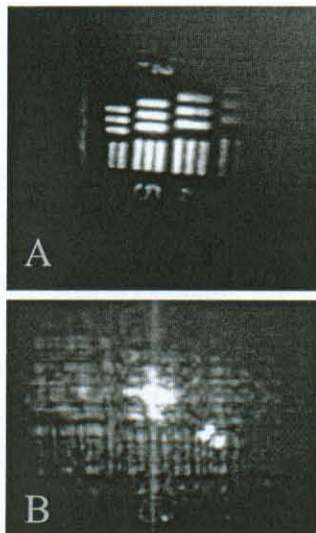


Figure 13. Edge enhancement result: (A) is the input image and (B) is the edge enhanced version

The experiment was performed on the low spectral band of the Fourier spectrum as shown in Figure 14. The clean reference beam overlapped only a small portion of the Fourier spectrum.

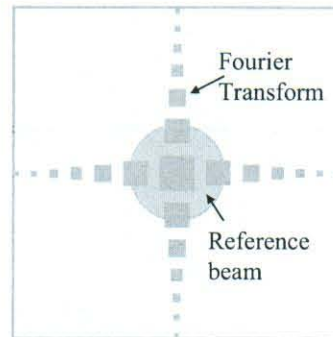


Figure 14. Reference beam covering the low spectral band of the Fourier spectrum

The reference information in this experiment is a delta function, therefore the input-output nonlinear transfer function can be expressed as equation 2, where  $a$  is the delta function Fourier transform adjusted by the beam amplitude.

$$A(v_x, v_y) = A(0) \left[ \frac{1 + m/(\lambda f_l)^2 |a + S(v_x, v_y)|^2}{1 + m/(\lambda f_l)^2 |a + S(v_x, v_y)|^2 \exp(-g)} \right]^{1/2} \quad (2)$$

We are currently in the process of implementing more complex image deconvolution schemes.

#### 4. CONCLUSION

In conclusion, we tested the fidelity of the two beam coupling energy transfer spatial light modulator for both imaging and Fourier processing systems. We have also tested the fidelity of the two beam coupling energy transfer as a symmetric joint Fourier processor. The dynamic range compression capability of the Nitto Denko organic film for noise compression and peak (signal) to noise ratio enhancement as well as edge enhancement via two beam energy transfer, which is essentially a special case of dynamic range compression deconvolution, were implemented.

**Acknowledgment:** We would like to acknowledge Dr. Lee from AFOSR for supporting this project and Dr. Yamamoto from Nitto Denko Technology for providing us with the organic photorefractive materials.

## REFERENCES

- (1) Rafael C. Gonzalez, Richard E. Woods, "Digital Image Processing," Prentice Hall (2002)
- (2) B. Haji-Saeed, S. K. Sengupta, W. D. Goodhue, J. Khoury, C. L. Woods, and J. Kierstead, "Spectrally variable two-beam coupling nonlinear deconvolution," *Appl. Opt.* 46, 8244-8249 (2007)
- (3) B. Haji-saeed, S. K. Sengupta, W. Goodhue, J. Khoury, C. L. Woods, and J. Kierstead, "Nonlinear dynamic range compression deconvolution," *Opt. Lett.* 31, 1969-1971 (2006)
- (4) J. Khoury, C. L. Woods, B. Haji-Saeed and J. Kierstead "Two-Beam Coupling Deconvolution via Spatially Variable Dynamic Spectral Compression," SPIE, Aerosense Conference Optical pattern recognition XVI (Orlando FL, 31 March - 1 April 2005) vol. 5816, pp. 277-283 (2005)
- (5) J. Khoury, M. Cronin-Golomb, P. Gianino, and C. Woods, "Photorefractive two-beam-coupling nonlinear joint-transform correlator," *J. Opt. Soc. Am. B* 11, 2167-2174 (1994)
- (6) Jed Khoury, Peter D. Gianino and Charles L. Woods, "Engineering aspects of the two-beam coupling correlator," *Optical Engineering* 39 (05), 1177-1183, (2000)
- (7) J. Khoury, M. Cronin-Golomb, A. M. Biernacki, and C. L. Woods, "Photorefractive phase-conjugate technique for measuring surface granularity," *Appl. Opt.* 33, 7655-7660 (1994)
- (8) J. Feinberg, "Real-time edge enhancement using the photorefractive effect," *Opt. Lett.* 5, 330- (1980)
- (9) D. M. Pepper, J. AuYeung, D. Fekete, and A. Yariv, "Spatial convolution and correlation of optical fields via degenerate four-wave mixing," *Opt. Lett.* 3, 7-9 (1978)
- (10) E. Ochoa, J. W. Goodman, and L. Hesselink, "Real-time enhancement of defects in a periodic mask using photorefractive Bi<sub>12</sub>SiO<sub>20</sub>," *Opt. Lett.* , 430-432 (1985)
- (11) G. J. Dunning, E. Marom, Y. Owechko, and B. H. Soffer, "All-optical associative memory with shift invariance and multiple-image recall," *Opt. Lett.* 12, 346-348 (1987)
- (12) H. Rajbenbach, A. Delboulbé, and J. P. Huignard, "Noise suppression in photorefractive image amplifiers," *Opt. Lett.* 14, 1275-1277 (1989)
- (13) A. E. T. Chiou and P. Yeh, "Beam cleanup using photorefractive two-wave mixing," *Opt. Lett.* 10, 621-623 (1985)
- (14) L.-J. Cheng, G. Gheen, T.-H. Chao, H.-K. Liu, A. Partovi, J. Katz, and E. M. Garmire, "Spatial light modulation by beam coupling in GaAs crystals," *Opt. Lett.* 12, 705-707 (1987)
- (15) H. Kogelnik, *Bell Syst. Tech. J.* 48, 2909 (1969)

(16) J. Khoury, Peter Gianino, Charles L. Woods "Is the two beam coupling correlator realizable" To appear in Asian Journal of physics.

(17) George Asimellis, "holographic implementation of nonlinear joint transform correlators," PhD thesis, Tufts University (1997)

(18) Michiharu Yamamoto, Nasser Peyghambarian , "Photorefractive composition," Patent Publication number: US 2006/0235163 A1,"

